ARTICLE

THE ANALYST www.rsc.org/analyst

Fast quantification of water in single living cells by near-infrared microscopy†

Erik Bründermann,[a] Andreas Bergner,[a] Frank Petrat,[b] Robert Schiwon,[a] Götz Wollny,[a] Ilona Kopf,[a] Herbert de Groot[b] and Martina Havenith[a]

[a] *Physical Chemistry II, Ruhr-University Bochum, Germany. E-mail: Erik.Bruendermann@rub.de; Fax: 49 234 3214183; Tel: 49 234 3224239*

[b] *Institute of Physiological Chemistry, Clinics of the University Essen, Germany. E-mail: frank.petrat@uni-essen.de; Fax: 49 201 7235943; Tel: 49 201 7234105*

Received 13th April 2004, Accepted 21st June 2004
First published as an Advance Article on the web 22nd July 2004

We have set up a near-infrared microscope using a tuneable diode laser in the range from 1530 to 1570 nm. This spectral range is close to the peak of the water overtone absorption. We used this new microscope to study liver cells, hepatocytes, showing that quantitative information of the intracellular water concentration in living cells can be extracted.

Introduction

Microscopic methods can determine the intracellular distribution of biomolecules like proteins and lipids. In fluorescence microscopy[1–3] it is often difficult to find a suitable fluorophor, *e.g.* due to spectral overlapping with cellular autofluorescence, photobleaching and/or cytotoxicity, assuring maintenance of cell viability and photochemical stability during prolonged and repetitive single-cell imaging.[4] In addition, the use of fluorescent probes bears the risk of affecting the physiological functions of the targeted molecules.

Infrared[5–9] (IR) and Raman[6,10–15] microscopy of living cells can provide a label free approach to detect the distribution of intracellular molecules using their specific absorption bands in the IR, the so-called ''fingerprint'' region, without the need to tag the molecules of interest.

Our experiments tackle the problem of the water distribution in living cells. Water is a small molecule impossible to tag with a fluorophor. However, it is the most abundant molecule in living organisms, the solvent for all biomolecules present in cells.

The intracellular water concentration and the cell volume are important parameters for cell function and its vitality. They may serve as a ''second message'' in the regulation of cellular function.[16] Oxidative stress, nutrients, hormones, insulin and glutamine, can alter the water concentration in cells leading to changes in osmotic pressure resulting either in cell swelling or shrinking. Persistent alterations of metabolism occur within minutes in response to aniso-osmotic cell volume changes. Effects of hypo-osmotic cell swelling on liver function have been associated[17] with an increase in protein synthesis, glycogen synthesis[18] and glutamine breakdown, whereas hyper-osmotic cell shrinkage can lead to an increase in proteolysis, glycogenolysis, and viral replication. Cell volume and its regulatory mechanism participate in the machinery leading to apoptotic and necrotic cell death; they may account for or contribute to clinical disorders such as hypercatabolism, fibrosing disease and altered neuroexcitability.[19] Chronic hepatic encephalopathy, for example, is linked to astrocyte swelling as an early event, although an increase in intracranial pressure is clinically not detectable.[17,19]

Water has strong infrared absorption bands. Infrared absorption measurements seem to us the most promising tool to accurately determinate the concentration of intracellular water to a high degree of precision. High-speed IR imaging can resolve dynamic effects like redistribution of intracellular water or water flux from extracellular to intracellular space and *vice versa*. In addition, high-speed imaging is necessary for rapid testing of living single cells upon drug delivery to determine therapeutic dosages.

The osmotic response of cells has been investigated with various methods like fluorescence,[20–22] NMR[23–25] and light scattering[26,27] techniques. In contrast IR imaging offers some major advantages over the previous mentioned techniques: The strong absorption of water in the IR combined with the good spatial resolution allows determining water mobility, distribution and content of single living cells in a quantitative manner without the need of labels or assumptions.

Experimental set-up

The absorption of the overtone band of water peaks at 1400 nm. To keep the experimental set-up simple and cheap we have chosen a laser with an emission band around 1550 nm for which laser telecommunication technology provides a multitude of components.

Fig. 1 shows the experimental set-up. A dichroic mirror (DM) and several mirrors (M1-M4) guide the two laser beams, a 632.822 nm Helium/Neon (HeNe) laser and a tuneable (1530–1570 nm) near-infrared (NIR) semiconductor laser (Sacher Lasertechnik, Germany) into a microscope objective (OB, 40×, NA = 0.65) on the same optical axis which is defined by two iris diaphragm spaced 3 meters apart. The optical system is easily aligned *via* the visible light source on which the invisible NIR light path can be overlaid using the two iris diaphragms. The HeNe laser is also used to compare NIR with visible images to determine cell features. The following measurements are made by alternatively using the NIR or HeNe laser source. The minimal achievable focus for this objective has a diameter of 0.59 μm (HeNe-laser) and between 1.4 and 1.5 μm (NIR laser), respectively. The living cells are prepared on a glass slide and placed inside an aquarium which can be filled with different solutions.

A lens (L1) with a focal length of 50 mm collects the transmitted light. The focal point of the lens coincides with the

† Presented at the 82nd International Bunsen Discussion Meeting on "Raman and IR Spectroscopy in Biology and Medicine", Jena, Germany, February 29–March 2, 2004.

DOI: 10.1039/b408954p

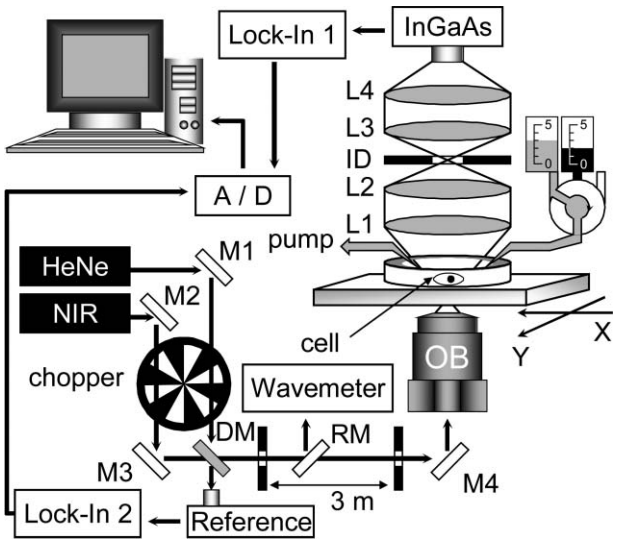

Fig. 1 Experimental set-up showing the two laser sources focused into the sample chamber, which is raster-scanned in the focal plane.

objective focus, which is 0.5 mm above the first lens surface of the objective. This leads to a parallel beam, again focused (L2) to pass through an inserted iris diaphragm (ID) to reduce stray light. Finally, the transmitted laser light is focused (L3, L4) on the 1 mm square detector surface of a single InGaAs detector, which has its maximum sensitivity in the range 1100–1700 nm with a 10-fold reduced sensitivity at 633 nm. Chopping the laser beams between 1 and 2 kHz and using a Lock-In technique improves the signal-to-noise ratio. An optional second detector using the small fraction of intensity of both lasers leaking at the dichroic mirror (DM) can register small fluctuations in laser power.

A motorized two-axis translation stage raster-scanned the sample chamber horizontally in the focal plane. A manually driven translation stage controlled by a micrometer screw adjusts the vertical (z-axis) position of the sample chamber. The sample is moving with constant velocity (''on-the-fly'' mode) scanning the rows in the focal plane stepping to a new position after each row. The ''on-the-fly'' mode is rather fast, so that the number of rows and the settling time of the translation stage after each row dominate the total scanning time.

The standard microscope objective leads to a reduced working distance by 0.29 mm in the NIR in comparison to the HeNe-laser. This value slightly varies by the amount of water in the sample chamber, as the refractive index close to the absorption will be wavelength depended. Correcting the vertical position by manually adjusting the translation stage with the sample chamber while scanning, gives the final position.

By using a removable mirror (RM) light can be directed into a wavemeter which measures the wavelength showing that both lasers were stable within at least 0.001 nm. Varying the NIR laser frequency it is possible to measure the wavelength dependent absorption coefficients of water and buffer. For example, we determined that the water absorption coefficient decreases with increasing wavelength from 15 to 10 cm^{-1}, for 1530 to 1570 nm respectively.

An analogue–digital interface (A/D) converted the signal for a computer. An in-house program based on LabView (National Instruments) selected the appropriate signal levels for each pixel, controlled the translation stages to 300 nm accuracy, and built an image.

The acquisition time for an image consisting of 500 by 500 pixels is about 16 min. On average, each pixel corresponds to a dwell time of 3.8 ms matched to the chopper frequency.

Animals

Male Wistar rats (200–350 g) were obtained from the central animal laboratory of the university clinics (Zentrales Tierlaboratorium, Universitätsklinikum Essen, Germany). Animals were kept under standard conditions with free access to food and water. All animals received humane care in compliance with the institutional guidelines.

Cell isolation and preparation

Hepatocytes were isolated and seeded on to glass cover slips of 0.1 mm thickness in 6-well cell culture plates, and cultured in L-15 medium supplemented with 5% (v/v) FCS, 2 mM L-glutamine, 8.3 mM glucose, 0.1% BSA, 14.3 mM $NaHCO_3$, 50 mg L^{-1} gentamicin and 1 μM dexamethasone (for details see ref. 4).

Experiments with hepatocytes were performed as early as 2 h up to 2 days after isolation of the cells. The glass coverslips were transferred to a sample chamber and cells were washed with HBSS at 37 °C. The sample chamber is insulated against leakage by a rubber ring below. A Teflon ring screws into the mount above the carrier, which allows covering the cells with solution. In all experiments, we took care to maintain a water layer of at least 2 mm (0.6 mL) above the cover slip surface to assure complete coverage of the cells. The water level height is given by a defined volume, filling the chamber of 20 mm diameter using an Eppendorf pipette with an accuracy of 2 μL.

Quantitative measurements were performed with single cells surrounded by void areas to allow subtraction of background absorption of the incubation buffer (Hank's balanced salt solution, HBSS, pH = 7.35). HBSS consists of 0.3% solvated ions and buffer molecules (HEPES = N-2-hydroxyethylpiperazin-N'-2-ethansulfonic acid) while water contributes 99.7%. An optional flow sample chamber can deliver fresh solution in order to control the pH level, to add or remove supplements and to exchange the complete incubation buffer.

Results

In primary studies, cells had been cultured on glass cover slips coated with collagen as a matrix, which is, however, not advisable for quantitative measurements due to the non-uniformity of the collagen-layer thickness. In addition, the collagen matrix layer cracked so that in the NIR image lines and interference pattern with high contrast appeared due to diffraction leading to long-range image distortion.

Measurements of cells without any mediator revealed several positive side effects: the cells are much less dense, which enabled us to simultaneously scan the cells and the buffer solution as reference. The reference measurement can be used to determine the water absorption of the buffer as well as to monitor intensity fluctuations of the laser. The measured absorption coefficient of the buffer solution provides an independent method to extract information on the solution height. Clustering of cells and stacked cells are mostly avoided allowing the unambiguously determination of the cell circumference. All images within this article display cells cultured without collagen.

Fig. 2 shows a hepatocyte two days after isolation. After two days the cell has lost its initial circular cross-section and is spread out onto the glass. The focus size of both lasers gives sufficient resolution to image cells and even the cellular nucleus.

Fig. 3 shows the transmission of hepatocytes in HBSS prepared with water (H_2O) or heavy water (D_2O). Note, that the image with D_2O as solvent has been measured second, which explains that some of the cells have changed or left their positions being washed away during the influx of the D_2O

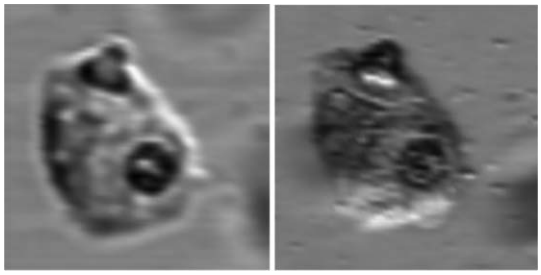

Fig. 2 Imaging of cultured rat hepatocytes at 1570 nm (left) and at 633 nm (right). Square images (0.12 mm) consisting of 60 by 60 pixels. Images shown are raw data – no post-processing has been used to improve contrast.

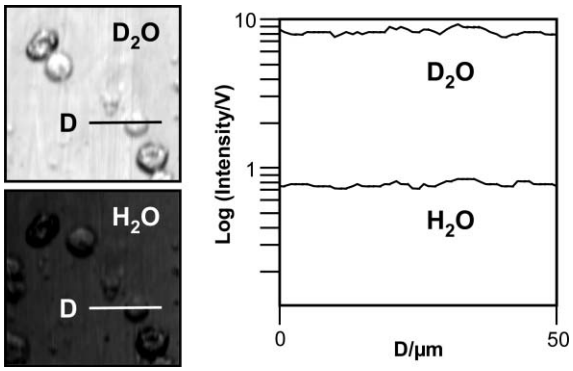

Fig. 3 NIR-images (1530 nm) of hepatocytes in buffer solutions using different solvents (H_2O and D_2O). The traces (D) indicate the signal level of the transmitted laser light measured by the detector in volts at the same lateral positions. Acquisition time for the square 0.15 mm images consisting of 150 by 150 pixels was 211 s each.

solvent. The absorption band of D_2O is red-shifted in frequency in comparison to the band of H_2O, so that a 10-fold increase of NIR laser transmission for the used layer thickness results. We expect that it is easily possible to study fast exchange processes and intracellular water flows due to the high contrast between H_2O and D_2O.[28] Other intracellular constituents are a constant background contributing (0.05 ± 0.02) cm^{-1} at 1530 nm. The long-term cytotoxicity of D_2O can be avoided in repetitive exchange experiments by returning to the buffer containing H_2O after each measurement since exchange processes will occur on short timescales between milliseconds and seconds.

We were able to demonstrate the dynamic changes in the water distribution in living cells by studying the swelling and shrinking of hepatocytes over time by diluting or concentrating the incubation buffer HBSS, respectively (*cf.*, Fig. 4). Each solution completely exchanged the previous one. We scanned the same section immediately thereafter to minimize the total measurement time. The time to scan each image was 212 s. More time in-between each scan could have reduced the wavy structure, which results from surface waves in the sample chamber induced during solution exchange amplified by the regular scanning motion. The last image shows shrinkage upon

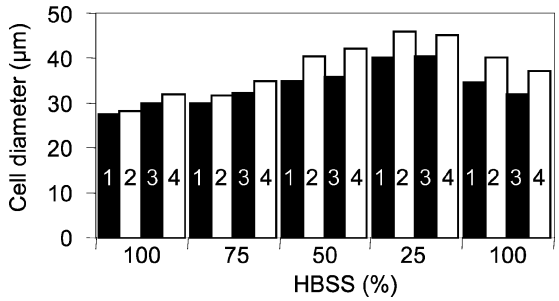

Fig. 5 Size of four cells taken from Fig. 4 as a function of the HBSS/water ratio ranging from 100% down to 25% and back to 100%.

reversal to the physiological HBSS. Fig. 5 summarizes size measurements of the four cells which stay within the image at all times.

Using $\alpha = -\ln(I/I_R)/L$ we can easily extract the water concentration if the thickness of the cell – the cell height L along the line of view – is known. I is the measured intensity at each pixel and I_R is a reference pixel intensity of the buffer in a void area. We can obtain this information by confocal imaging and adding up the different slices. Our current NIR microscope does not have a confocal capability. To test the principal method we have used a commercial confocal laser-scanning microscope (LSM 510, Zeiss, Germany) equipped with an argon laser to excite the fluorescent dye calcein at 488 nm detecting fluorescence above 505 nm. We measured several calcein-stained cell shapes 2–5 h after isolation by confocal sectioning. They exhibit a near circular cross-section if projected along the normal of the cover slip surface. Fig. 6 shows a typical shape. The result of the measurements is a diameter-to-height ratio of 0.8. The standard deviation of 0.2 represents physiological differences between individual cells. For an individual cell the diameter-to-height ratio stays rather constant even during swelling. Table 1 shows the measured diameter of a swelling cell and the involved cell heights using a strict diameter–height relation with the ratio of 0.8.

Choosing one cell, as an example, we can calculate the surplus transmission averaging a few pixels from the centre part of the cell. The excess transmission (see Table 1) was measured due to the lower intracellular water concentration in comparison to the extracellular buffer along the intracellular height L in comparison to a buffer column of the same height. The contribution by the water column above the cell can be removed by dividing through an image reference pixel containing only buffer solution. The accuracy of the absorption measurement is within 1%. The measurement of the diameter and the confocal slicing has been done with an accuracy of approximately 1 μm. Since the surplus emission is due to changes of both parameters, cell volume and intracellular water concentration, we can further separate the contributions tentatively by using the diameter–height-ratio. We found that the cell volume increases monotonously by at least a factor of three during dilution of the buffer to 25%. The intracellular water concentration, however, changed by a much more

Fig. 4 Effects of hypo-osmolarity on the morphology of cultured hepatocytes imaged with NIR microscopy (1530 nm). Each 0.15 mm square image consists of 150 by 150 pixels. HBSS buffer was diluted with pure water (ratios from left to right: 100% HBSS, HBSS/water = 3:1–75% HBSS, 2:2–50% HBSS, 1:3–25% HBSS, back to pure HBSS).

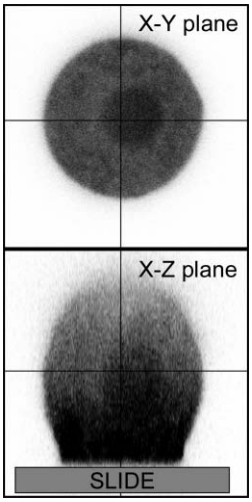

Fig. 6 Cross-sections of an isolated hepatocyte made visible by the fluorescent dye calcein in a laser-scanning microscope. The base of the cell (indicated by the slide) is about 20 μm wide expanding to a round cross-section at maximum diameter. Sedimentation of the fluorophor can be observed. The upper image is a view from the top onto the cell and sample slide; the lower image is a side view assembled from approximately 1 μm thick confocal slices.

Table 1 NIR (1530 nm) excess transmission and other parameters of cell 1 of Fig. 5 for the HBSS dilution sequence

HBSS	100%	75%	50%	25%	100%
NIR excess	3.9%	0.6%	3.2%	13%	7.4%
Diameter/μm	28	30	35	40	35
Height/μm	35	38	44	50	43

complex pattern. The initial drop of excess transmission to 0.6% indicates a very diluted concentration of intracellular biomolecules, which seem to concentrate again for further dilution, suggesting the onset of protein synthesis and subsequent relative reduction of intracellular water. An absolute very accurate quantification of the water concentration is now in reach if we can simultaneously measure the absorption and the cell height by NIR confocal sectioning of the same cell.

Conclusion and outlook

We have demonstrated that it is possible to quantify the water concentration in dynamical processes by using a cheap diode laser source and a simple NIR microscope. NIR microscopy can provide qualitative and quantitative information on the water distribution in living cells. Confocal sectioning of a cell for which the absorption is measured will allow the absolute quantification of the water concentration. Since the contrast in our NIR microscope is very high we could integrate a NIR confocal capability into our current set-up. This modification will allow accurate calculations of each individual cell height without staining or assumptions on a diameter-height-ratio. Medical applications that study the effects of drugs on osmolarity of whole cells are possible despite the limited spatial resolution.

Technological advances can speed up image acquisition, reduce artefacts, improve sensitivity and temporal resolution. Acousto-optical deflectors and laser mirrors on galvo-drives can speed up image acquisition by scanning the laser beam instead of the sample chamber, which will reduce or even remove water surface waves. For very fast image acquisition we can benefit from cheap and advanced technology in telecommunications. NIR lasers in the frequency band around 1550 nm can be modulated up to several gigabits reducing possible pixel dwell times to nanoseconds.

Recently, InGaAs cameras[29] have become commercially available and may remove the need for scanning. We have observed that the water influx into cells under osmotic pressure occurs within tens of milliseconds for which video image speeds of 30 to 50 Hz might be sufficient.

A two-color detection method might boost sensitivity. Spectroscopic gas sensors use two frequencies with one frequency tuned to the absorption peak of a molecule while detuning the other frequency off-peak.

High temporal resolution combined with high sensitivity will allow us to follow the physiological changes due to the water distribution on the milliseconds to seconds timescale in detail, which may enable new therapeutic strategies.

Acknowledgement

We acknowledge support by the Ministry of Science and Research of North Rhine Westfalia.

References

1 W. Denk, J. H. Strickler and W. W. Webb, *Science*, 1990, **248**, 73.
2 M. Straub, P. Lodemann, P. Holroyd, R. Jahn and S. W. Hell, *Eur. J. Cell Biol.*, 2000, **79**, 726.
3 A. Egner, S. Jakobs and S. W. Hell, *Proc. Natl. Acad. Sci.*, 2002, **99**, 3370.
4 F. Petrat, D. Weisheit, M. Lensen, H. de Groot, R. Sustmann and U. Rauen, *Biochem. J.*, 2002, **362**, 137, and references within; F. Petrat, H. de Groot, R. Sustmann and U. Rauen, *Biol. Chem.*, 2002, **383**, 489.
5 N. Jamin, P. Dumas, J. Moncuit, W.-H. Fridman, J.-L. Teillaud, G. L. Carr and G. P. Williams, *Proc. Natl. Acad. Sci.*, 1998, **95**, 4837.
6 J. R. Mourant, R. R. Gibson, T. M. Johnson, S. Carpenter, K. W. Short, Y. R. Yamada and J. P. Freyer, *Phys. Med. Biol.*, 2003, **48**, 243.
7 M. Diem, S. Boydston-White and L. Chiriboga, *Appl. Spectrosc.*, 1999, **53**(4), 148A–161A.
8 N. Jamin, P. Dumas, J. Moncuit, W. H. Friedman, J.-L. Teillaud, G. L. Carr and G. P. Williams, *Cell. Mol. Biol.*, 1998, **44**(1), 9.
9 M. Miljkovic, M. Romeo, C. Matthäus and M. Diem, *Biopolymers*, 2004, **74**, 172.
10 N. Uzunbajakava, A. Lenferink, Y. Kraan, E. Volokhina, G. Vrensen, J. Greve and C. Otto, *Biophys. J.*, 2003, **84**, 3968.
11 A. Zumbusch, G. R. Holtom and X. S. Xie, *Phys. Rev. Lett.*, 1999, **82**, 4142.
12 J.-X. Cheng, Y. K. Jia, G. Zheng and X. S. Xie, *Biophys. J.*, 2002, **83**, 502.
13 X. Nan, J. Cheng and X. S. Xie, *J. Lipid Res.*, 2003, **44**, 2202.
14 J. Cheng, A. Volkmer, L. D. Book and X. S. Xie, *J. Phys. Chem. B*, 2002, **106**, 8493.
15 G. J. Puppels, T. C. Bakker Schut, N. M. Sijtsema, M. Grond, F. Maraboeuf, C. G. de Grauw, C. G. Figdor and J. Greve, *J. Mol. Struct.*, 1995, **347**, 477.
16 G. J. Puppels, F. F. M. de Mul, C. Otto, J. Greve, M. Robert-Nicoud, D. J. Arndt-Jovin and T. M. Jovin, *Nature*, 1990, **347**, 301.
17 D. Häussinger, *Biochem. J.*, 1996, **313**, 697.
18 A. Baquet, L. Hue, A. J. Meijer, G. M. van Woerkom and P. J. M. Plomp, *J. Biol. Chem.*, 1990, **265**(2), 955.
19 Y. Feng, V. Müller, B. Friedrich, T. Risler and F. Lang, *Wien Klin. Wochenschr.*, 2001, **113**(13–14), 477.
20 M. Zelenina and H. Brismar, *Eur. Biophys. J.*, 2000, **29**, 165.
21 M. Yano, R. A. Marinelli, S. K. Roberts, V. Balan, L. Pham, J. E. Tarara, P. C. de Groen and N. F. LaRusso, *J. Biol. Chem.*, 1996, **271**(12), 6702.
22 A. S. Verkman, *J. Membrane Biol.*, 2000, **173**, 73.
23 G. Bacic, J. C. Alameda, Jr, A. Iannone, R. L. Magin and H. M. Swartz, *Magn. Reson. Imaging*, 1989, **7**, 411.
24 S. Ratkovic, *Scientia Yugoslavica*, 1981, **7**, 19.
25 J. Pfeuffer, U. Flögel and D. Leibfritz, *NMR Biomed.*, 1998, **11**, 11.
26 M. Echevarria, *J. Gen. Physiol.*, 1992, **99**, 573.
27 M. McManus, J. Fischbarg, A. Sun, S. Hebert and K. Strange, *Am. J. Physiol.*, 1993, **265**, C562.
28 E. O. Potma, W. P. de Boeij, P. J. M. van Haastert and D. A. Wiersma, *Proc. Natl. Acad. Sci. USA*, 2001, **98**, 1577.
29 R. S. Jones, G. D. Huynh, G. C. Jones and D. Fried, *Opt. Express*, 2003, **11**, 2259.